

# Supplementary material for

## Section 3.1 Climatic Drivers

September 15, 2016

*Lead Authors: Peter Lang Langen (Danish Meteorological Institute); Patrick Grenier (Ouranos); Ross Brown (Environment and Climate Change Canada)*

This supplementary section presents a more detailed description of some of the physical mechanisms driving Arctic regional climate change presented in section 3.1 and discusses projections for additional variables of the hydrological cycle (other than precipitation). This section also includes supplementary figures and tables referred to in the main text.

In the following, section numbering follows that in the main text such that, for instance, SM3.1.1 provides additional information related to Section 3.1.1. Not all sections in the main text have supplementary information and these section numbers are skipped here.

### **SM3.1.1 Global and Arctic climate change**

#### *Arctic amplification*

Arctic amplification of warming (AAw) can be defined mathematically as the ratio of the Arctic to the global surface warmings (Bracegirdle and Stephenson, 2013; Barnes and Polvani, 2015). In climate model simulations, it emerges from a variety of complex and intertwined feedbacks. There is no consensus for the exact decomposition of the feedbacks involved and their relative importance for AAw (Langen et al. 2012; Taylor et al., 2013). It is important to note that the feedbacks involved in AAw are not necessarily positive (i.e. acting to enhance temperature changes); a negative feedback (i.e. acting to damp temperature changes) may increase the AAw if it acts more strongly in the tropics than in the Arctic. In the next paragraph, we briefly describe these feedbacks, following the order of importance suggested by Pithan and Mauritsen (2014).

The Planck feedback corresponds to an increase in the longwave radiation (LWR) emission by a warming material (air, snow, bedrock, etc.). Because emitted LWR scales with the fourth power of surface temperature, Arctic surfaces must warm more than tropical surfaces to compensate for the same amount of additional LWR energy from the anthropogenic greenhouse effect. Another intertwined mechanism is the lapse-rate feedback, namely the response of the vertical temperature profile to the GHG forcing. In the Arctic, surface inversions limit vertical mixing, thus confining surface-based warming to the lowest part of the troposphere, whereas in the tropics, extra energy is more efficiently mixed via the release of latent heat in the upper troposphere. From a surface perspective, this corresponds to a warming feedback from the atmosphere which is larger in the Arctic relative to elsewhere. Another important mechanism contributing to AAw is the albedo feedback whereby additional absorption of shortwave radiation (SWR) from declining sea ice and snow cover enhances warming at the surface. Other feedbacks with smaller effects on AAw exist, and at least one mechanism opposes AAw, namely the water vapour feedback (warmer air tends to contain more water vapour, which is a GHG). It is important to note that the relative

importance of these mechanisms for the AAw evolve from one season to another. For example, the albedo feedback is almost inoperative during winter (although its main impact is an increased transfer of heat from the sea to the atmosphere during autumn and early winter), whereas the LWR feedbacks have a minimal effect during summer. In total, the Arctic amplification of the warming is more a cold-season than a warm-season phenomenon, as observed for the recent period (Serreze and Barry, 2011) and simulated for the late 21st century (Barnes and Polvani, 2015).

As for the warming, Arctic moistening is expected to be amplified relative to that at lower latitudes (Vihma et al. 2015). Actually, Arctic amplification of the moistening (AAM) is difficult to detect in recent observations (Zhang et al. 2012) but emerges in simulations for the 21st century (Kattsov et al. 2007). The hypothesis of an intensified global water cycle is based on the Clausius-Clapeyron (C-C) relationship between air temperature and the maximal amount of water vapour air can contain, which indicates an increase of 7 % per degree of warming (Held and Soden, 2006). Contrary to specific humidity (in grams of vapour per kilogram of air), precipitation is not expected to scale with the C-C relationship (Bengtsson et al. 2011), and a large spatial differential could occur, with Arctic and global mean precipitation sensitivities of 4.5 % and 1.6–1.9 % per degree of warming, respectively (Bintanja and Selten, 2014). As with AAw, the mechanisms contributing to AAM are complex and intertwined, and there is no consensus on their relative importance (Zhang et al., 2012; Kattsov et al. 2007). Moreover, the relative importance can vary through time. For example, analysis of simulations suggests that the relative importance of moisture transport to Arctic precipitation will decline with climate warming over the twenty-first century, even if in absolute terms moisture transport towards the Arctic will increase (Bintanja and Selten, 2014). Declines in sea ice cover contribute to AAM via increased local evaporation especially during autumn (Screen et al., 2013); this phenomenon has no equivalent at lower latitudes.

### **SM3.1.2 Atmosphere**

#### *Seasonal temperature projections*

Figures SM3.1 and SM3.2 show likely patterns for winter (December-January-February) and summer (June-July-August) average near-surface air temperature change relative to 1986-2005. The interpretation is the same as for changes in annual temperature (see section 3.1.2.1).

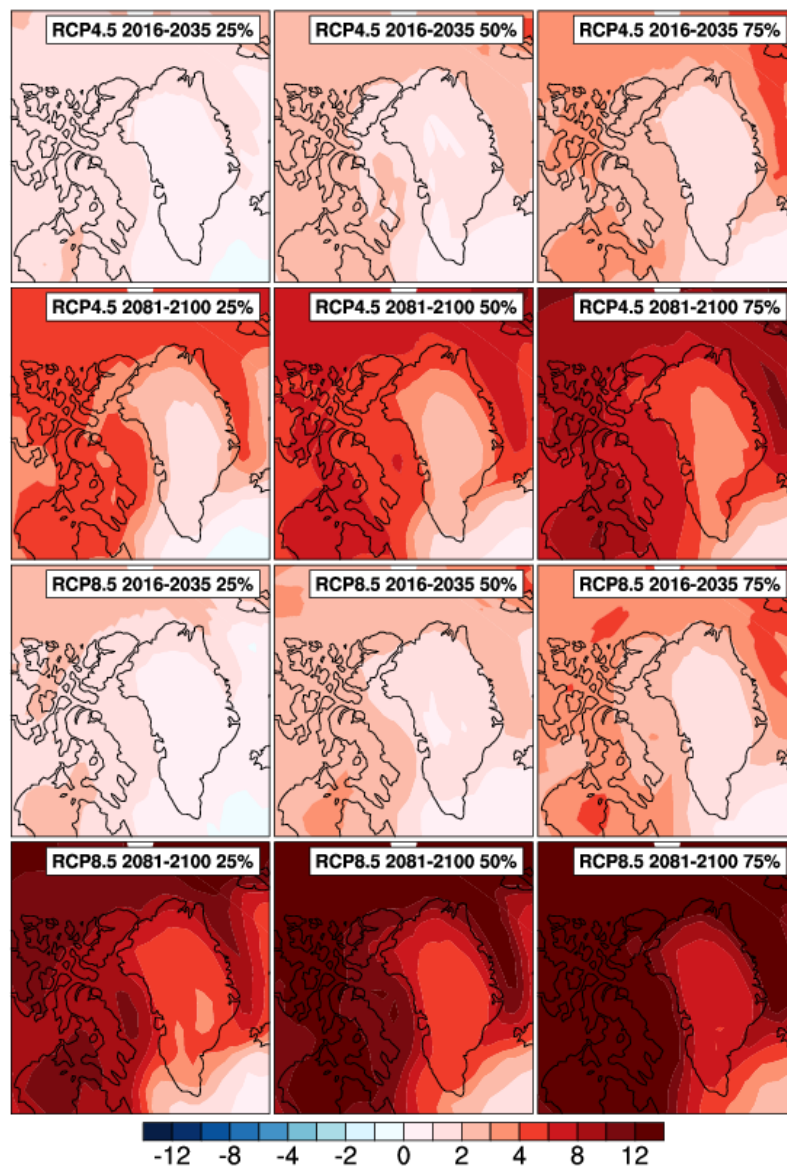


Figure SM3.1: Same as Figure 3.3, but for winter (December-January-February) temperature. Source of the data: IPCC (2013; Annex 1) [Prepared by Rasmus A. Pedersen, DMI]

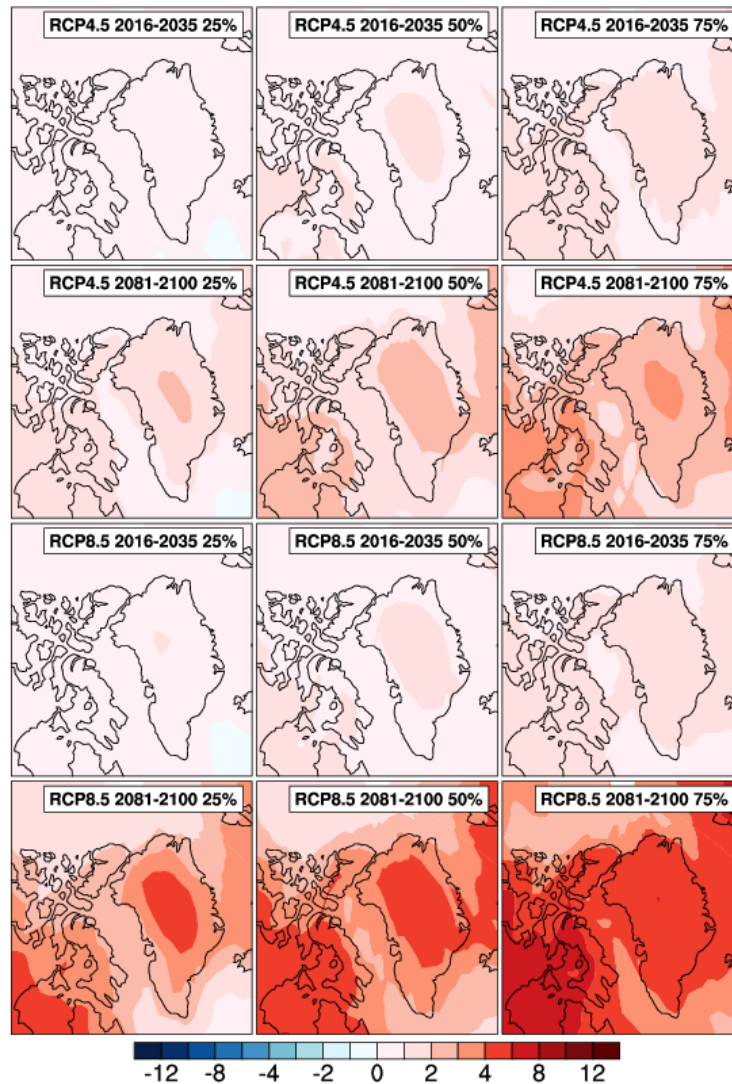


Figure SM3.2: Same as Figure 3.3, but for summer (June-July-August) temperature. Source of the data: IPCC (2013; Annex 1) [Prepared by Rasmus A. Pedersen, DMI]

#### *Projections for other variables of the water cycle*

Precipitation and humidity are probably the most investigated variables describing the atmospheric branch of the water cycle. But other important hydrological cycle variables may change as well. For example, using one global climate model, Bengtsson et al. (2011) have estimated that evaporation (E) north of 60°N should increase by about 20 % from the period 1959-1990 to the period 2069-2100, compared with a 25 % increase in precipitation (Pr). Bengtsson et al. (2011) also obtain an increase in the difference [Pr-E] of 28 % between the same periods [the Arctic is already a region of net water vapour convergence, with  $Pr-E > 0$  (Kattsov et al. 2007; Koenigk et al. 2013)]. The direction of these changes is in agreement with results from Kattsov et al. (2007), Vavrus et al. (2009), and Koenigk et al. 2013. The enhancement in Arctic moisture convergence is expected to cause an increase in river discharge (Zhang et al., 2012) and in groundwater storage (Muskett and Romanovsky, 2009), although not everywhere due to concurrent phenomena such as permafrost thawing. Also, natural large-scale oscillations can create periods of temporary decrease in precipitation and river discharge for some regions (Déry and Wood, 2005). Net Arctic Ocean freshening is

another expected consequence of the increase in [Pr-E] (Bintanja and Selten 2014; Koenigk et al. 2013), and is also subject to natural oscillations. This freshening will in turn potentially affect the ocean stratification and circulation, thus feeding back to the Arctic climate system (Davies et al. 2014; Kattsov et al. 2007). It must be stressed that there is considerable inter-annual variation in the Arctic hydrological cycle, and that no trends are discernible in the recent past transport of moisture into the Arctic based on ERA-Interim data (Bengtsson et al. (2011).

In addition to their role in the hydrological cycle, clouds are important for their direct impact on surface incoming short and longwave radiation. During winter clouds warm the surface through the greenhouse effect, whereas during summer they act to cool the surface from reflection of sunlight (Key et al. 2004; Koenigk et al. 2013). At the end of the 21st century over the BBDS region, CMIP3 GCMs driven by a SRES-A1B emission scenario show an increase in cloud amount with a multi-model average ranging from about 0 to 8 percentage points (depending on the season and location) compared with the end of the 20th century, and with inter-model standard deviations of the same order of magnitude (Vavrus et al. 2009). These results are also found for most of the Arctic Ocean and surrounding seas (except notably the North Atlantic sector), and Vavrus et al. (2009) link them with a projected reduction in sea ice concentration and an increase in sea surface evaporation. However, using an CMIP5 ensemble and a different methodology, English et al. (2015) conclude that cloud amount is not projected to change significantly over any Arctic surface type. Koenigk et al. (2013) found widespread reductions in Arctic cloudiness of about 10 % (5 %, 2 %) for RCP8.5 (RCP4.5, RCP2.6) during autumn from an analysis of EC-Earth model simulations, explained by warming dominating the increased specific humidity (leading to a decrease in relative humidity). These divergent results illustrate the large uncertainty in cloud cover change projections (Eisenman et al. 2007). Clouds are among the most challenging elements of the climate system to simulate, and this is particularly true for Arctic low-level mixed-phase clouds (English et al. 2015). Even from an observational viewpoint, Arctic cloud cover is difficult to characterize (Koenigk et al. 2013) as it does not fit well into the WMO standard cloud classification (Curry et al. 1996; Key et al. 2004).

#### **SM3.1.3.1 Snow**

Snow cover is a dominant feature of the landscape in the BBDS region with a seasonal snow cover present from early October to mid-June based on daily snow depth observations made at Canadian climate stations (Table SM3.1). Point snow depth observations made at climate stations may not be representative of surrounding areas but there is good agreement between estimates of variability in annual snow cover duration (SCD) over the Canadian land sector of the BBDS region from the surface observations and the NOAA satellite record (Figure SM3.3). The results provide evidence of a ~3 week decrease in the duration of snow on the ground since 1950. There are large uncertainties in trends in SCD and snow depth over the region across datasets related to different resolutions, different periods of data coverage and limitations of observations (e.g. cloud cover for satellite-based estimates of snow cover extent). This is clearly demonstrated in Figure SM3.4 which contrasts annual SCD trends from the 190.5 km NOAA satellite record with trends from the Liston and Hiemstra (2011) snow cover reconstruction from a physical snowpack model driven with 10-km downscaled reanalysis fields.

Table SM3.1: Snow cover climatology for Canadian stations in or adjacent to the BBDS region with at least 15 years of complete daily snow depth data in the 1981-2010 period. Data are from Brown and Braaten (1998) updated with daily snow depth in the EC climate archive. Source: ArcticNet IRIS-2 report (Brown et al. 2016 in press.)

Name	Lat (°N)	Long (°W)	Mean start date of continuous snow cover*	Mean end date of continuous snow cover*	Mean annual # days with snow cover^	Mean annual maximum snow depth (cm)	Mean date of annual max snow depth
Alert	82.5	-62.3	Sep-08	Jun-30	298.6	48.7	Apr-11
Arctic Bay	73.0	-84.6	Sep-13	Jun-22	282.3	39.4	Mar-28
Cape Dorset	64.2	-76.5	Oct-09	Jun-19	254.7	69.2	Apr-30
Chesterfield Inlet	63.3	-90.7	Oct-29	Jun-04	219.5	n/a	n/a
Clyde	70.5	-68.5	Sep-28	Jun-25	272.3	57.5	Apr-29
Coral Harbour	64.2	-83.4	Oct-13	Jun-16	247.8	46.8	Mar-29
Eureka	80.0	-85.9	Sep-23	Jun-09	263.3	20.3	Mar-26
Hall Beach	68.8	-81.2	Oct-07	Jun-24	261.9	51.8	Apr-20
Igloolik	69.4	-81.8	Oct-06	Jun-12	251.5	40.1	Apr-20
Iqaluit	63.7	-68.5	Oct-15	Jun-08	241.4	44.4	Mar-21
Pelly Bay	68.5	-89.8	Oct-07	Jun-13	250.7	71.3	Apr-20
Pond Inlet	72.7	-78.0	Sep-27	Jun-06	253.0	34.6	Feb-02
Rankin Inlet	62.8	-92.1	Oct-21	Jun-07	229.2	46.6	Apr-11
Resolute	74.7	-95.0	Sep-16	Jun-22	280.6	30.9	Mar-12
Taloyoak	69.6	-93.6	Oct-04	Jun-19	259.3	33.7	Apr-26
Whale Cove	62.2	-92.6	Nov-04	Jun-02	211.9	n/a	n/a
15-station regional average	69.4	-82.8	Oct-05	Jun-15	254.9	45.4	Apr-05

\* Defined as the first (last) date in the year with 14 consecutive days of snow depths  $\geq$  ( $<$ ) 2 cm.

^ Day with  $\geq$  2 cm snow on ground.

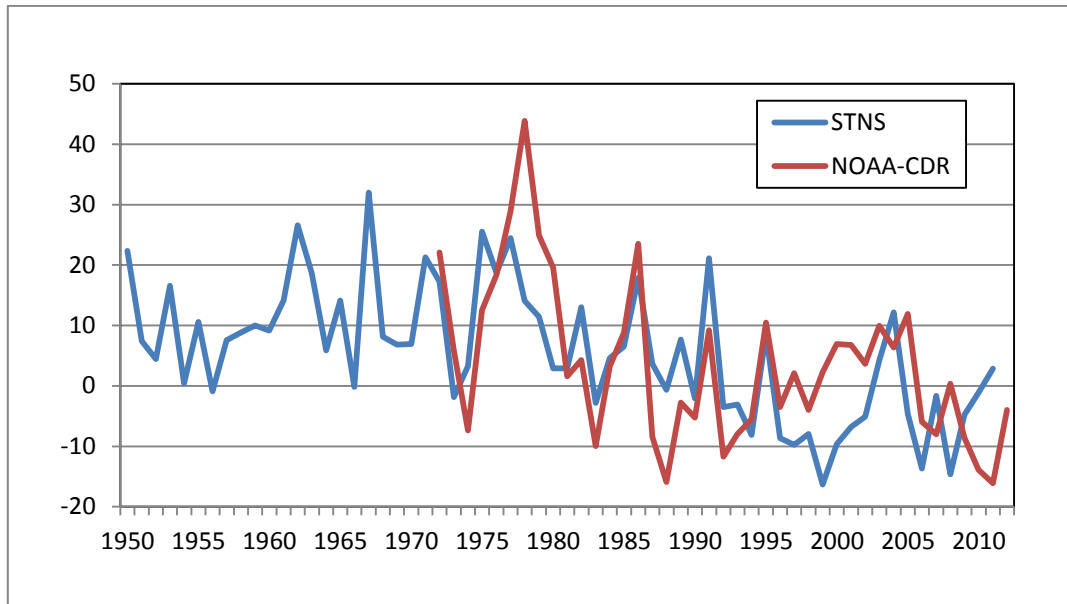


Figure SM3.3: Regionally-averaged anomalies (days) in annual snow cover duration from surface stations (STNS) and the NOAA-CDR satellite dataset (Estilow et al. 2015) over the Canadian land sector of the BBDS region. Anomalies are computed with respect to a 1981-2010 reference period. [Source: ArcticNet IRIS-2 report (Brown et al. 2016 in press)]

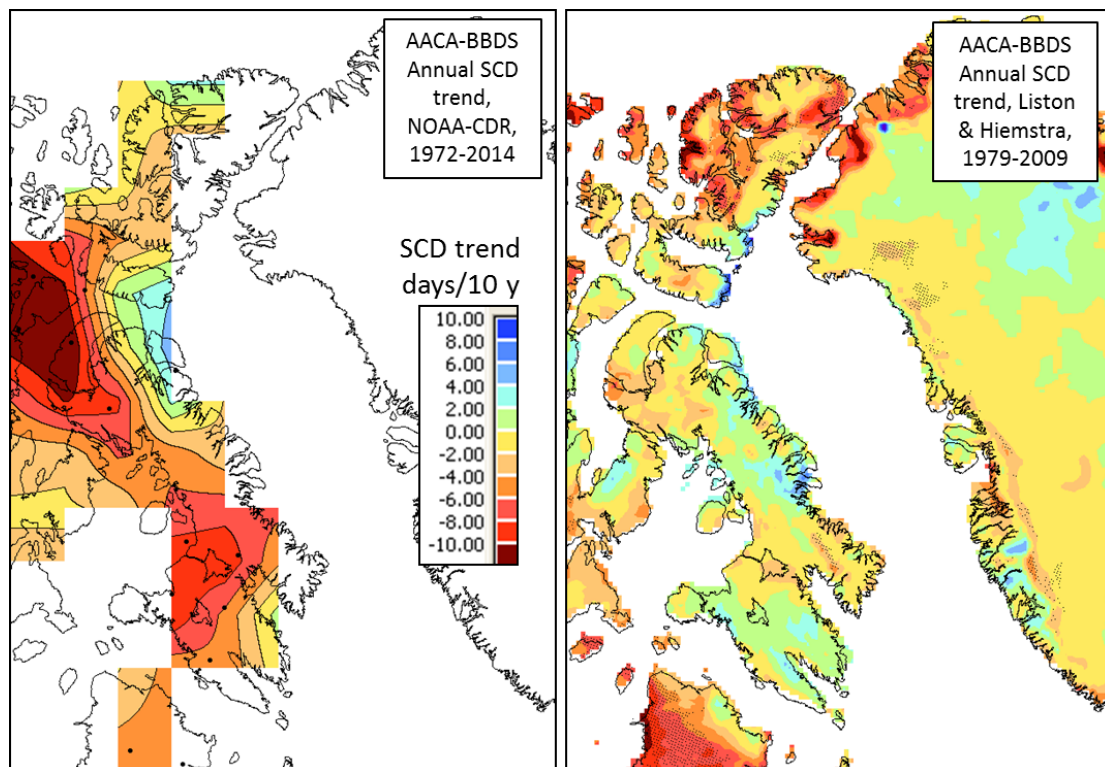


Figure SM3.4: Trend (days/10y) in annual snow cover duration (number of days with snow cover each year) estimated from the (a) NOAA CDR (Estilow et al. 2015) and (b) Liston and Hiemstra (2011) datasets. Note the different time periods covered by each dataset. The solid dots in the NOAA plot signify locally significant trends at the 0.05 level. [Prepared by Ross Brown, EC]



***Projected change in SWE<sub>max</sub> (%) relative to 1986-2005 period for 16 CMIP5 models, rcp4.5 (glacier mask applied)***

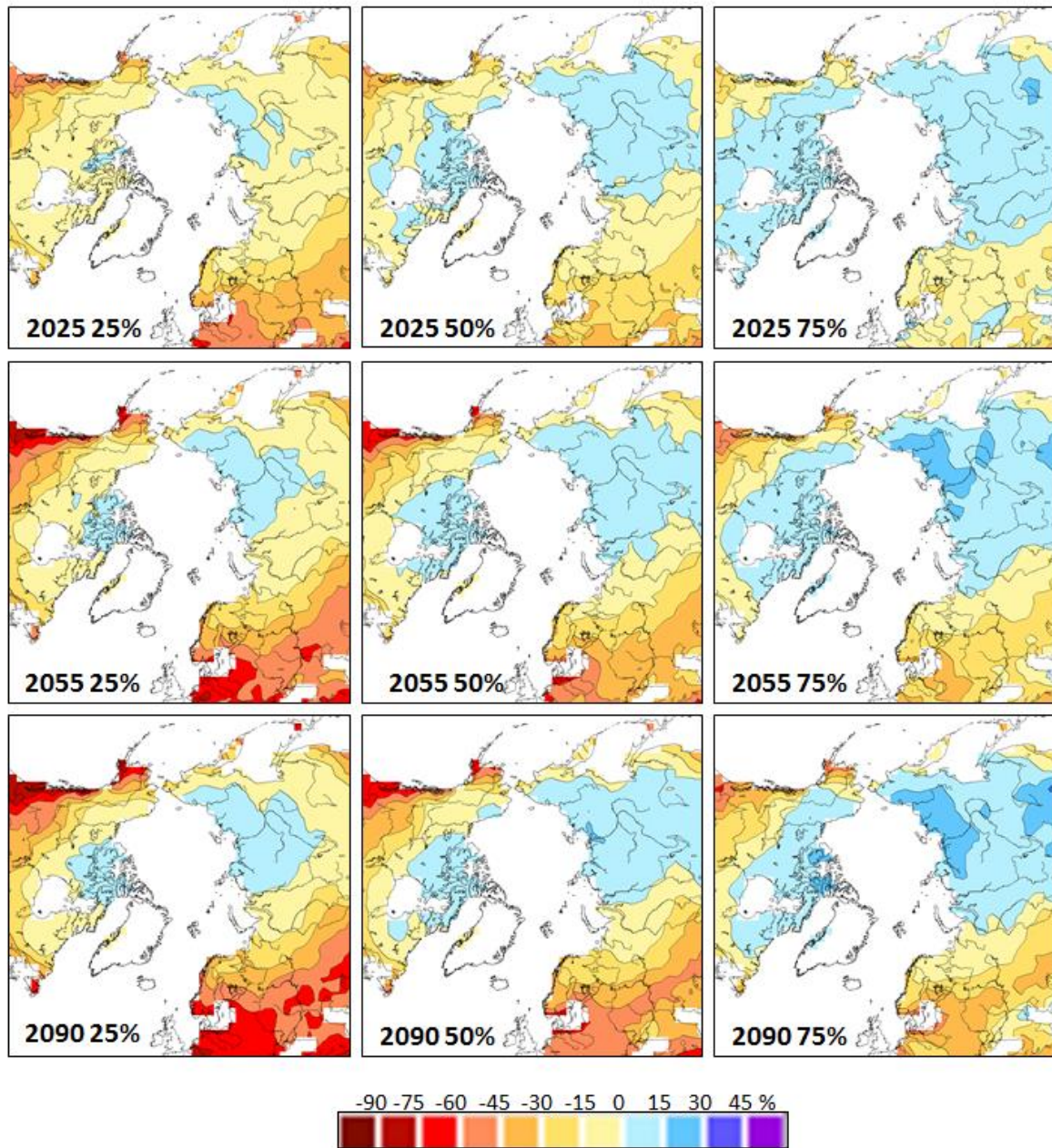


Figure SM3.5: Projected relative (%) change in mean annual monthly maximum SWE from 16 CMIP5 models for emission scenario RCP4.5. Results are shown for the median (50%) and upper (75%) and lower (25%) quartiles. 2025 corresponds to the 2016-2035 average, 2055 to the 2046-2065 average, and 2090 to the 2081-2100 average. [Source: SWIPA update report (Brown et al. 2017 in press)].



***Projected change in SWE<sub>max</sub> (%) relative to 1986-2005 period for 16 CMIP5 models, rcp8.5 (glacier mask applied)***

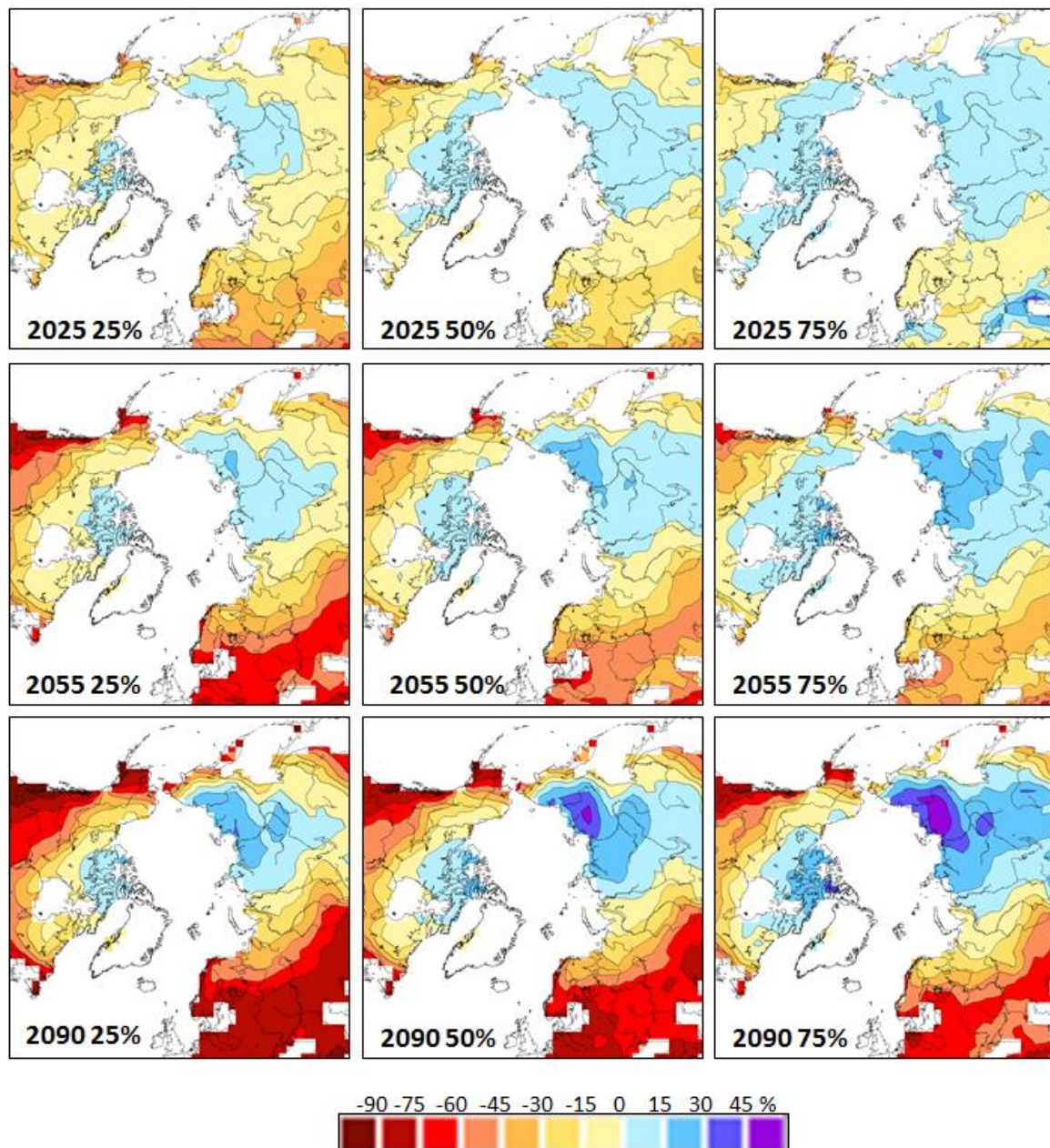


Figure SM3.6: Same as Figure SM3.5, but for emission scenario RCP8.5. [Source: SWIPA update report (Brown et al. 2017 in press)].

***Projected change in annual SCD (%) relative to 1986-2005 period  
for 16 CMIP5 models, rcp4.5***

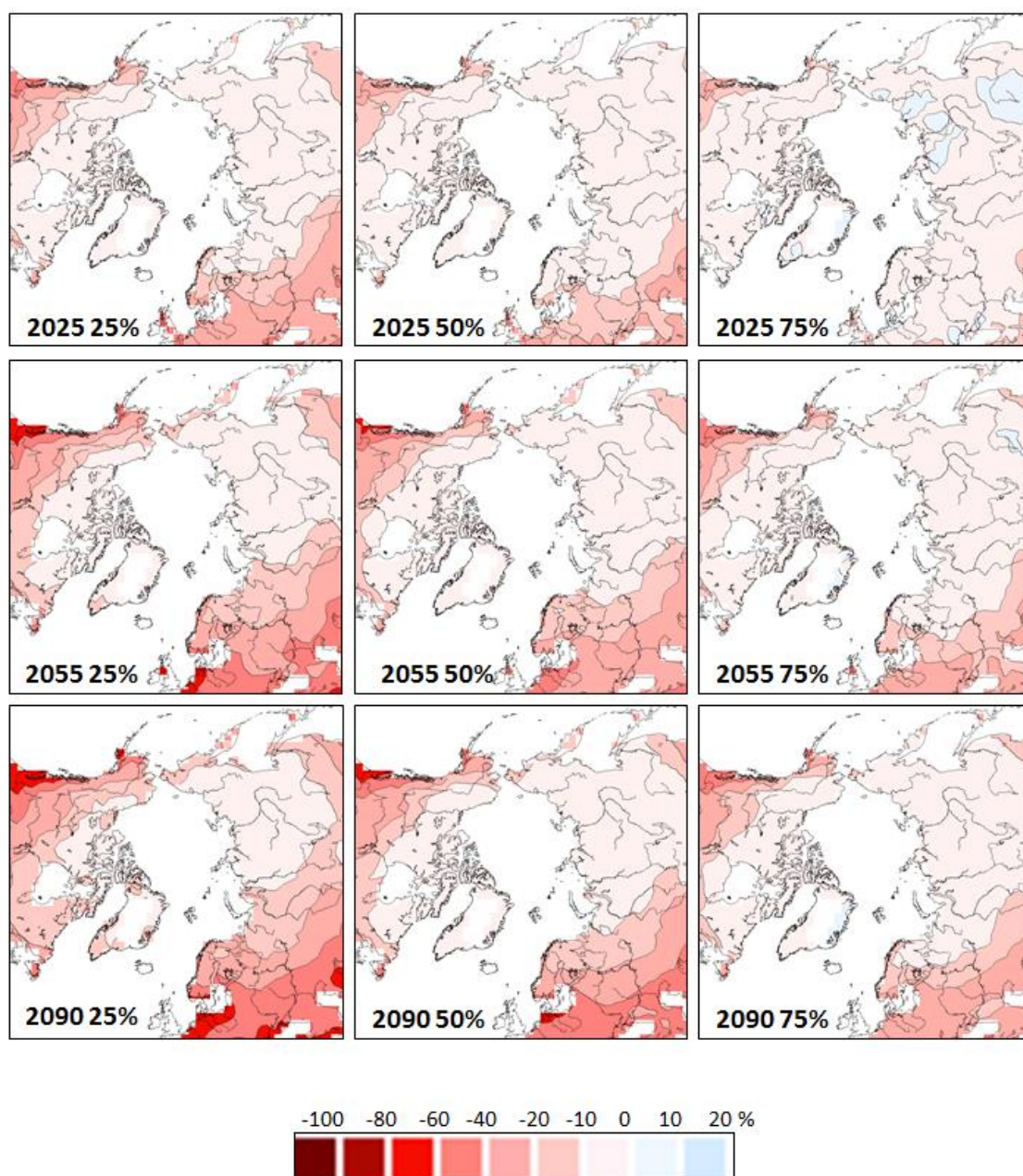


Figure SM3.7: Projected relative (%) change in mean annual SCD from 16 CMIP5 models for emission scenario RCP4.5. Panel organization follows Figure SM3.5. [Source: SWIPA update report (Brown et al. 2017 in press)].



***Projected change in annual SCD (%) relative to 1986-2005 period  
for 16 CMIP5 models, rcp8.5***

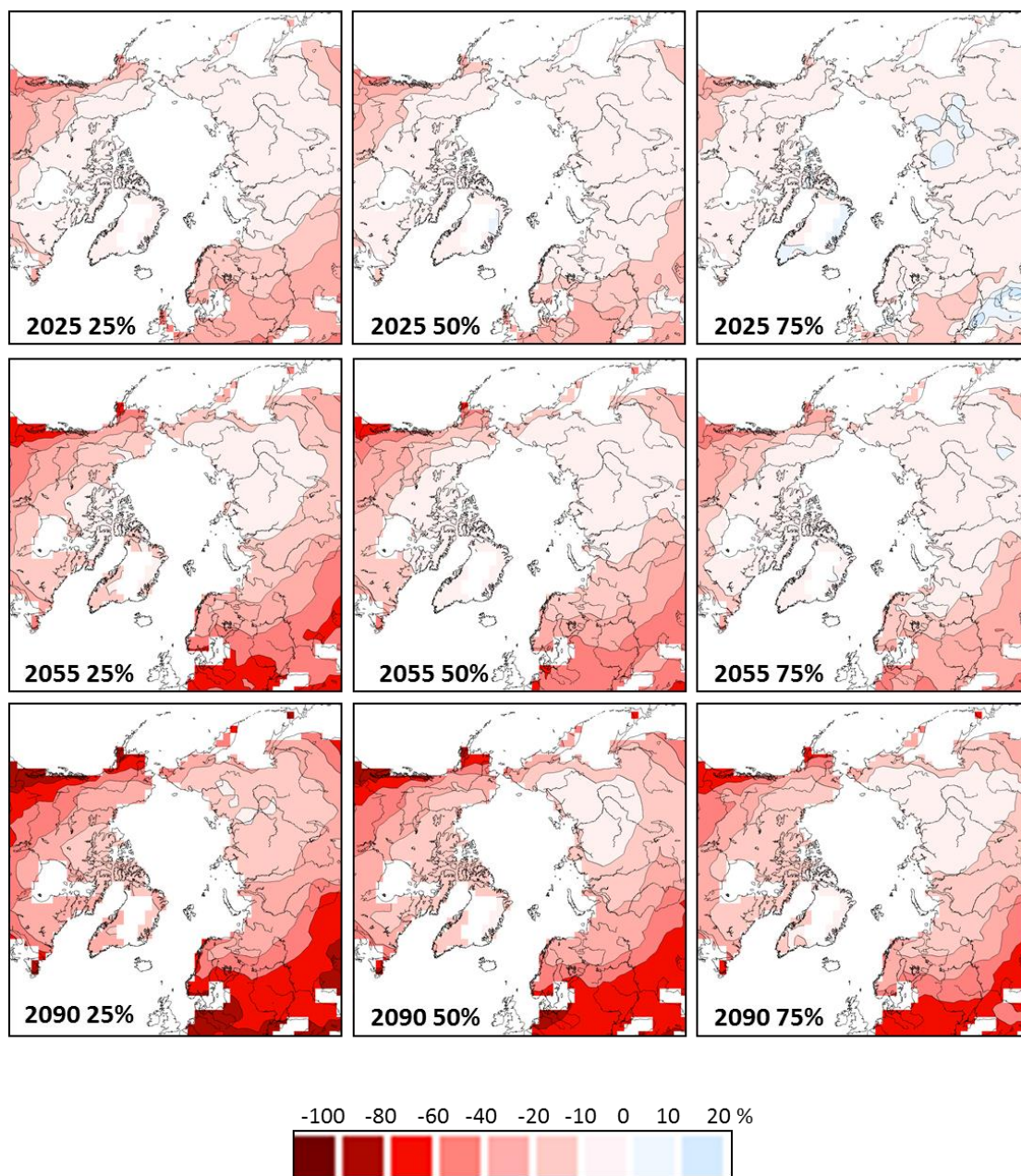


Figure SM3.8: Same as Figure SM3.7, but for RCP8.5. [Source: SWIPA update report (Brown et al. 2017 in press)].

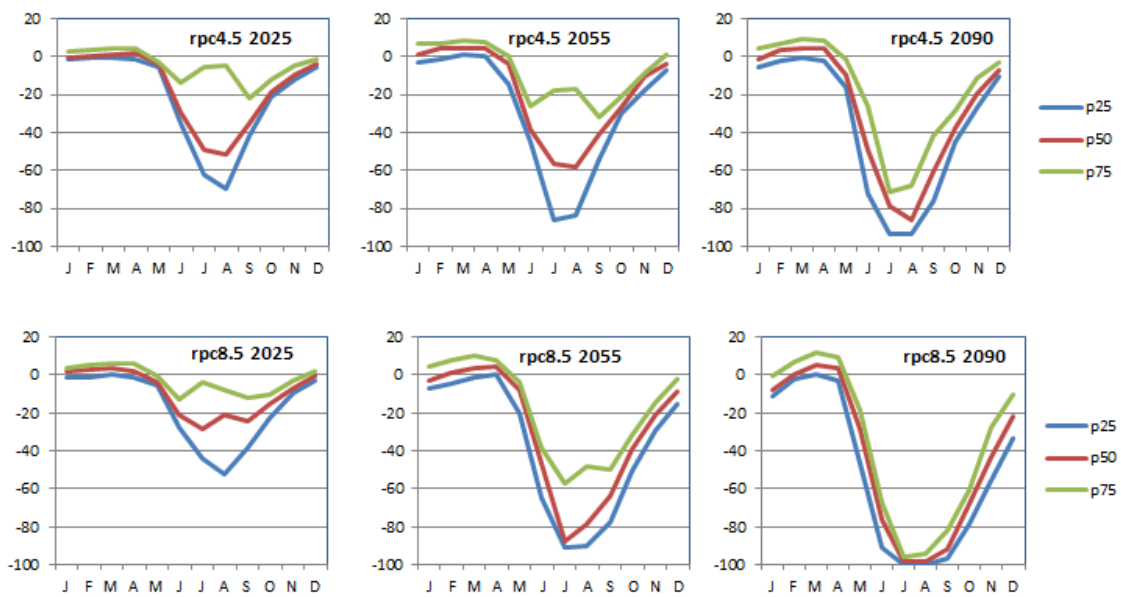


Figure SM3.9. Evolution of projected change (%) in monthly SWE over BBDS non-glacier land areas (25, 50 and 75% percentiles of 16 CMIP5 model runs) for RCP4.5 and RCP8.5. Change units are the % difference of 20-year periods with respect to the 1986-2005 average from the historical experiment simulations. The lines p25, p50 and p75 correspond to the median and lower and upper quartiles from the 16 model ensemble. The 20-year averaging periods used were: 2025 (2016-2035), 2055 (2046-2065), 2090 (2080-2099). [Prepared by Ross Brown, EC]

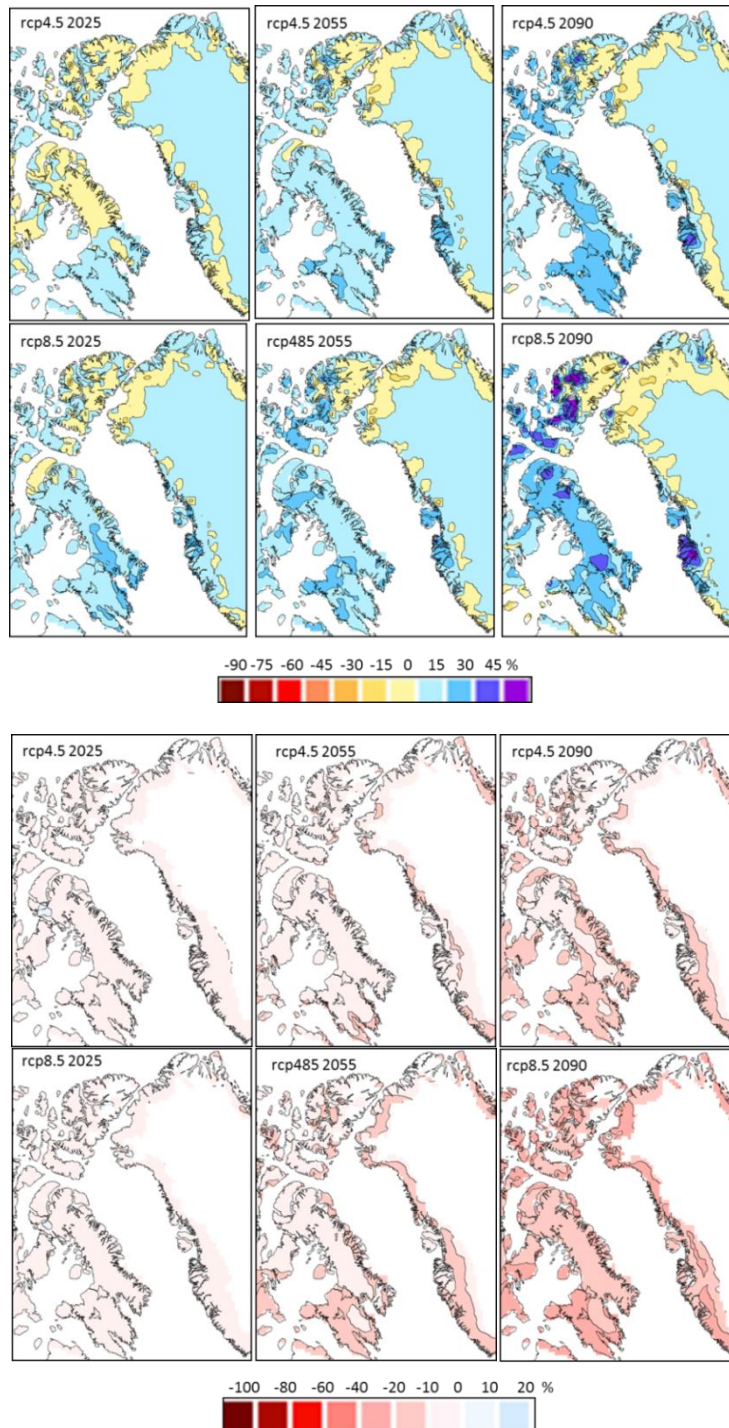


Figure SM3.10: Projected relative (%) changes in SWEmax (top) and annual SCD (bottom) over the BBDS region from the CanRCM4 regional climate model driven by the CanESM2 earth system model. SCD change is not computed over points with permanent snow cover. The glacier mask was not applied to CanRCM4 SWEmax changes as this destroys the spatial continuity of the field. The southern limit of the CORDEX Arctic domain crosses the northern tip of Ungava peninsula. [Prepared by Ross Brown, EC]

#### SM3.1.4 Ocean

There are three principal inputs of freshwater to the Baffin Bay: CAA passages, the West Greenland Current and the Greenland Ice Sheet. Section 3.1.4.1 discusses the mean values and relative contributions of these inputs. As also discussed there, variability plays a significant role and as an illustration, Figure SM3.11 provides an example from Barrow Strait of the seasonal and interannual variability of the transport through Barrow Strait.

Section 3.1.4.3 discusses projected changes in the strength of near-surface currents for the two periods 2016-2035 and 2081-2100 relative to 1986-2005 for the RCP8.5 scenario for three global models. Here we show in Figure SM3.12 the same but for the cooler RCP4.5 scenario.

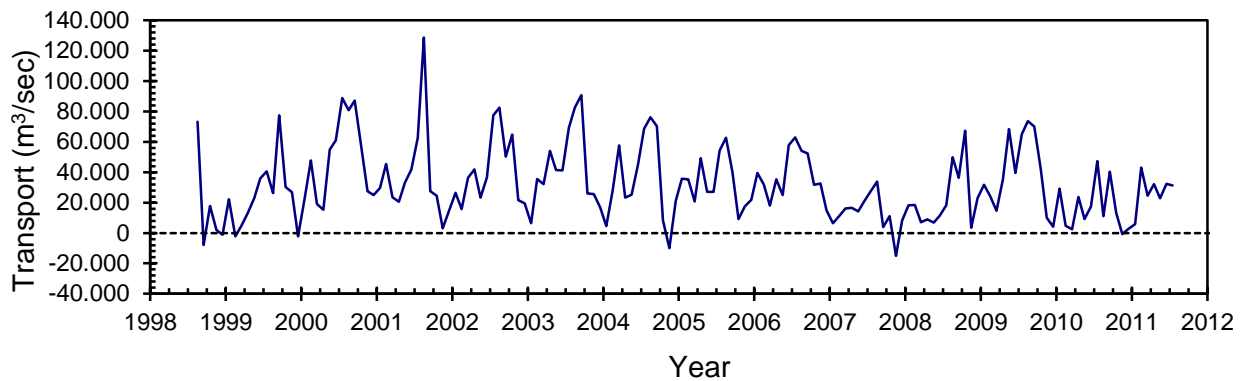


Figure SM3.11: Thirteen year time series of freshwater transport through Barrow Strait from instrumented mooring data. [Source: Peterson et al. (2012)].



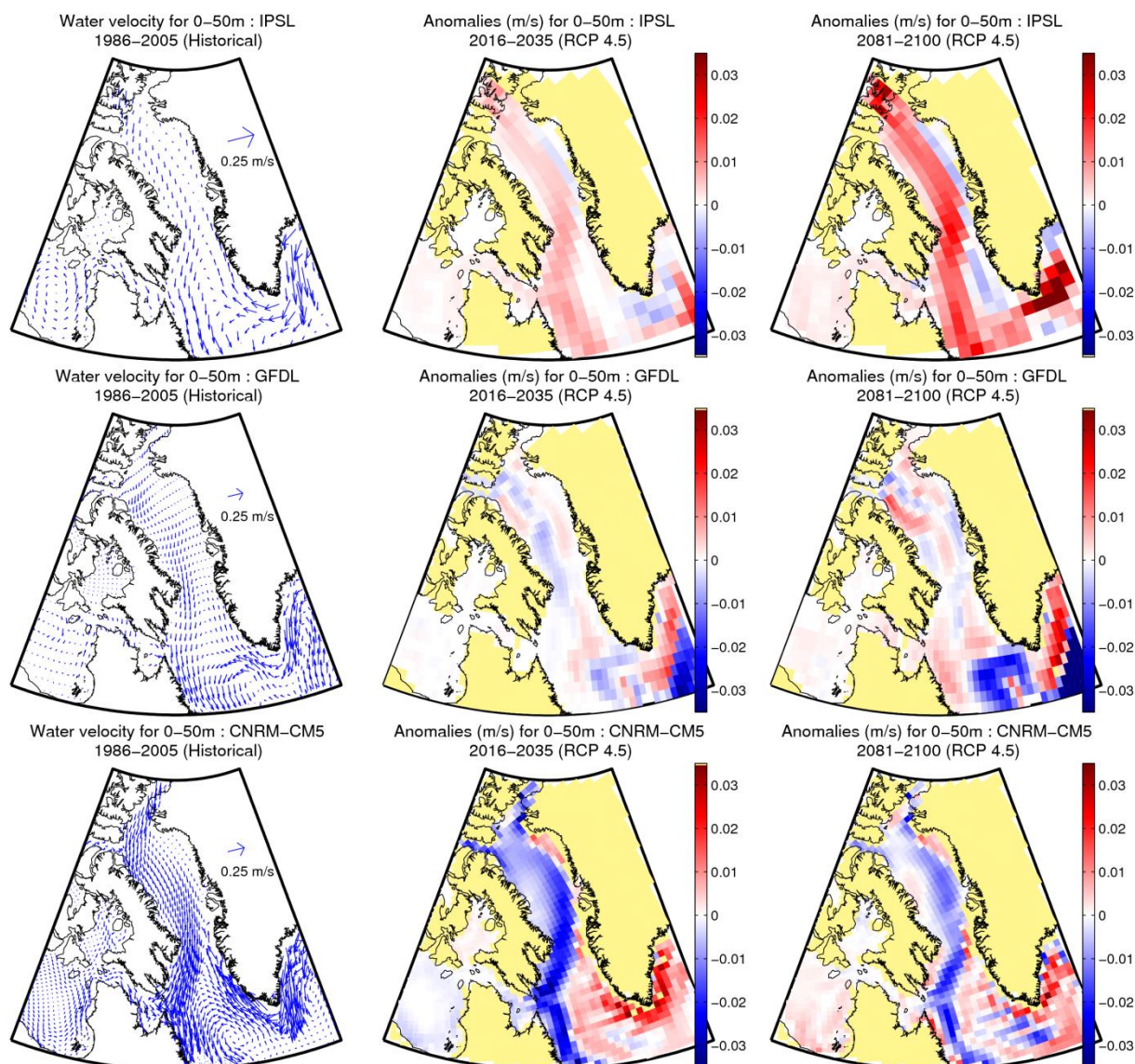


Figure SM3.12: Same as Figure 3.16, but for RCP4.5 emission scenario. [Prepared by Nicolas Lambert, Maurice-Lamontagne Institute, Fisheries and Oceans Canada]

### SM3.1.5 Sea ice

As discussed in Section 3.1.5.1, the BBDS region has experienced a 20% loss in July-November sea ice extent over the period from 1981-2014 (Figure SM3.13), with most of the change occurring in the period after 1998. 2006 had the lowest ice cover in the period of regular satellite observations.

With respect to landfast ice, Yu et al. (2014) documented a -4.5%/decade decrease in winter landfast ice area over Baffin Bay over the 1976-2007 period which was not statistically significant. However, their Baffin Bay regional time series of winter landfast ice area (Figure SM3.14) shows a ~50% reduction in landfast ice extent over the period from 1994 to 2005.

Section 3.1.5.2 discusses projected changes in sea ice concentration and thickness and shows multi-model ensemble projections of these quantities for RCP4.5 in fall (SON) and winter (DJF) in Figures 3.20 and 3.21. Here we show, in Figures SM3.15-SM3.20, the same for all four seasons, and for the three scenarios RCP2.6, RCP4.5 and RCP8.5.

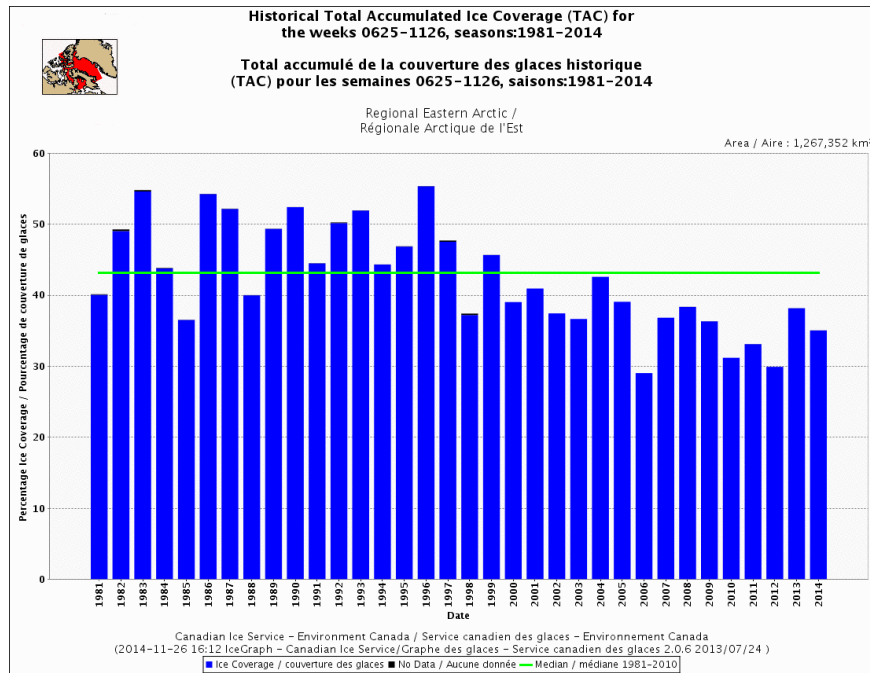


Figure SM3.13: July-November sea ice cover (%) over the Eastern Canadian Arctic region (red area on inset map) for the period 1981-2014. The green line is the median ice extent from 1981-2010. [Source: Canadian Ice Service (<http://ice-glaces.ec.gc.ca/App/WsvPrdCanQry.cfm?CanID=11090&Lang=eng>)]

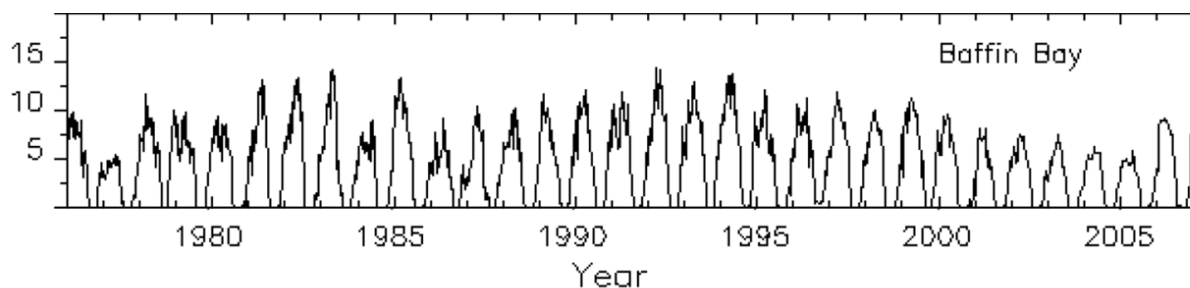


Figure SM3.14: Time series of weekly landfast ice thickness extent (104 km<sup>2</sup>) for the Baffin Bay region. [Source: Yu et al. (2014)]

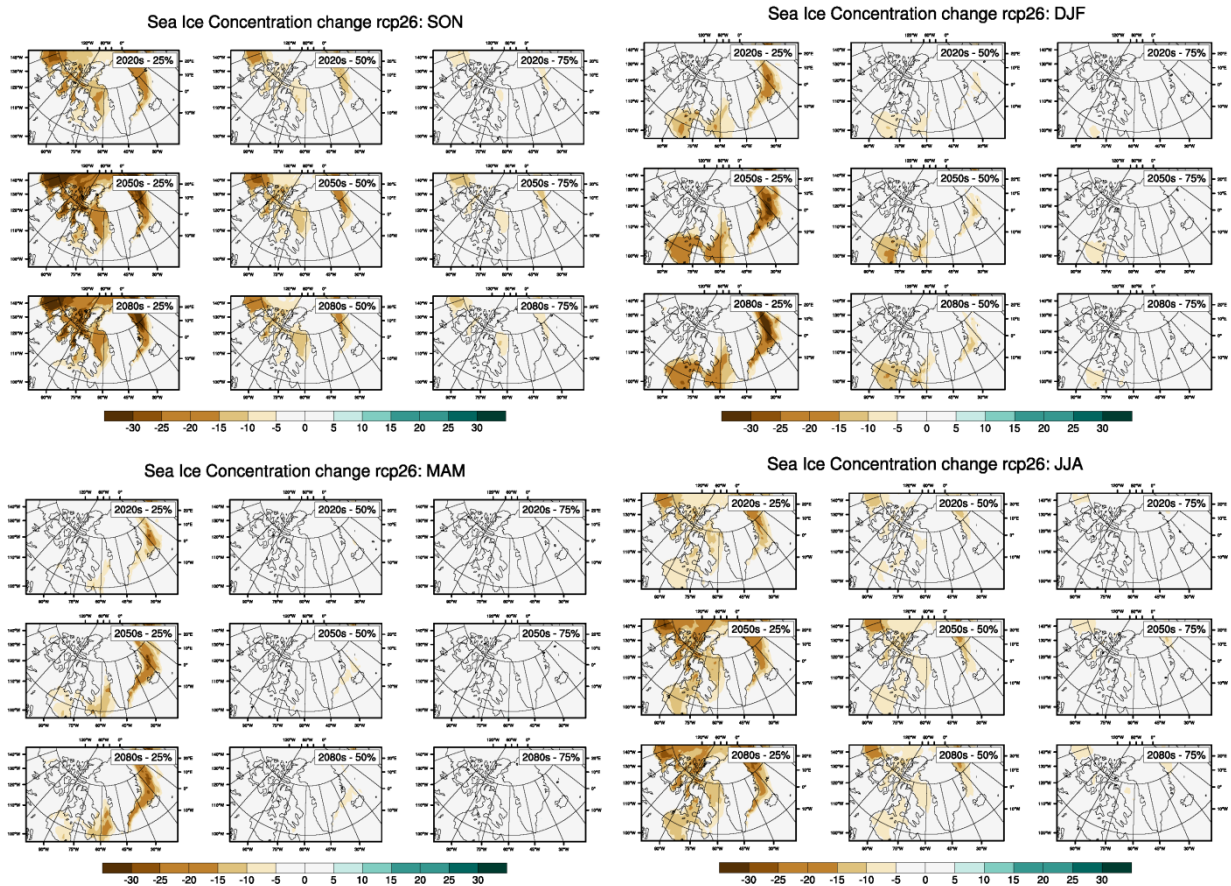


Figure SM3.15: 29 member CMIP5 multi-model projected change in seasonal sea-ice concentration (change in % concentration relative to 1986-2005 average) for RCP2.6 scenario. Results are shown for three periods in the future: 2016-2035 (labelled 2020s), 2046-2065 (labelled 2050s) and 2081-2100 (labelled 2080s), and illustrate the 25th, 50th and 75th percentile changes projected by the 29 CMIP5 models used (see BCB report for listing of models). [Prepared by Robin Rong, EC/CCCma]



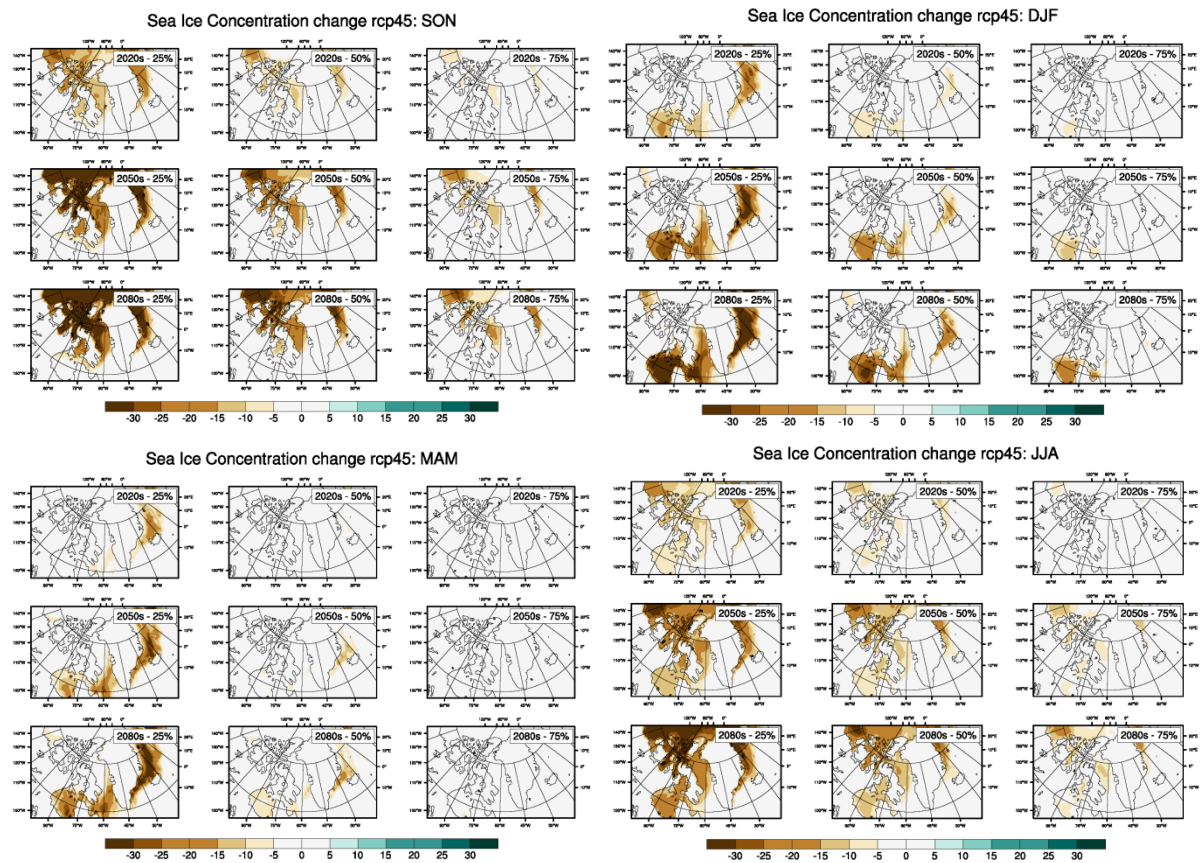


Figure SM3.16: Same as Figure SM3.15 for RCP4.5 scenario. [Prepared by Robin Rong, EC/CCma]

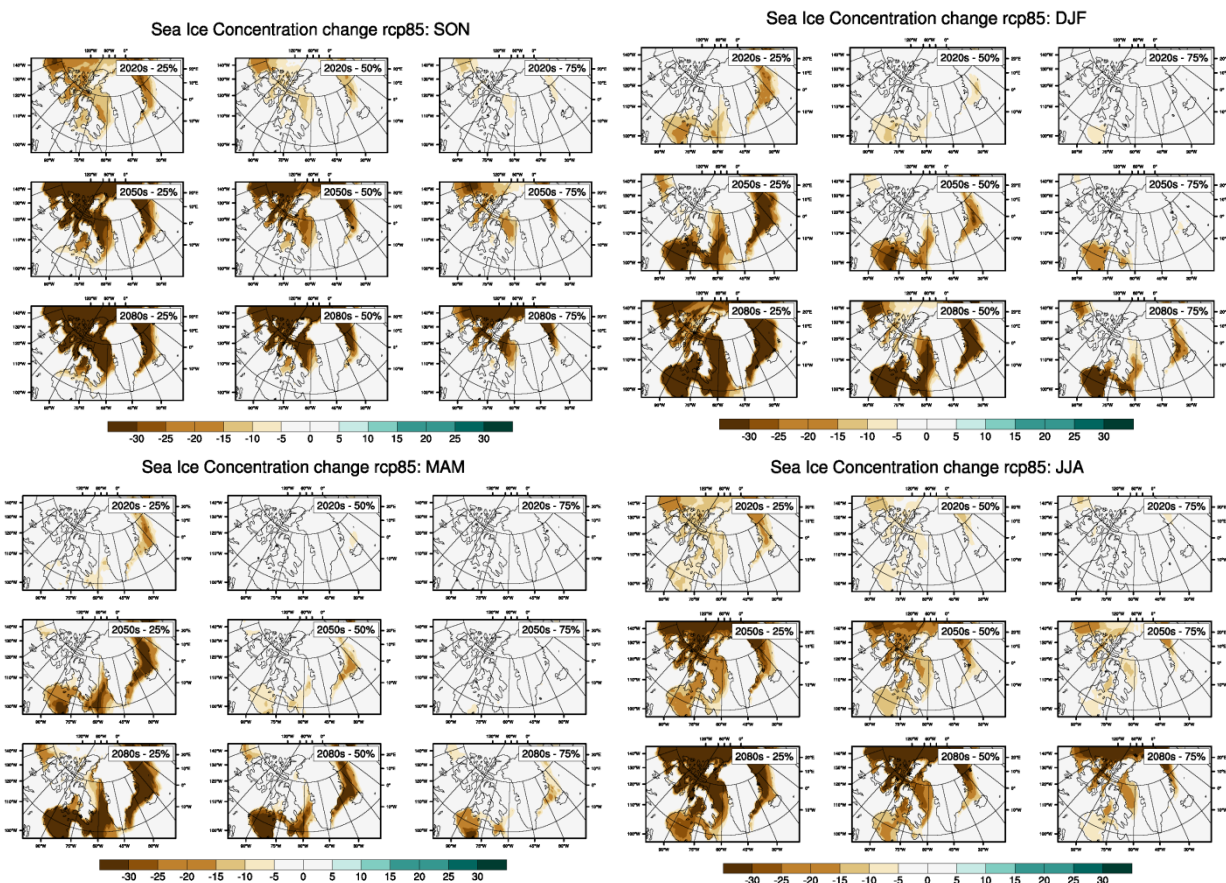


Figure SM3.17: Same as Figure SM3.15 for RCP8.5 scenario. [Prepared by Robin Rong, EC/CCma]

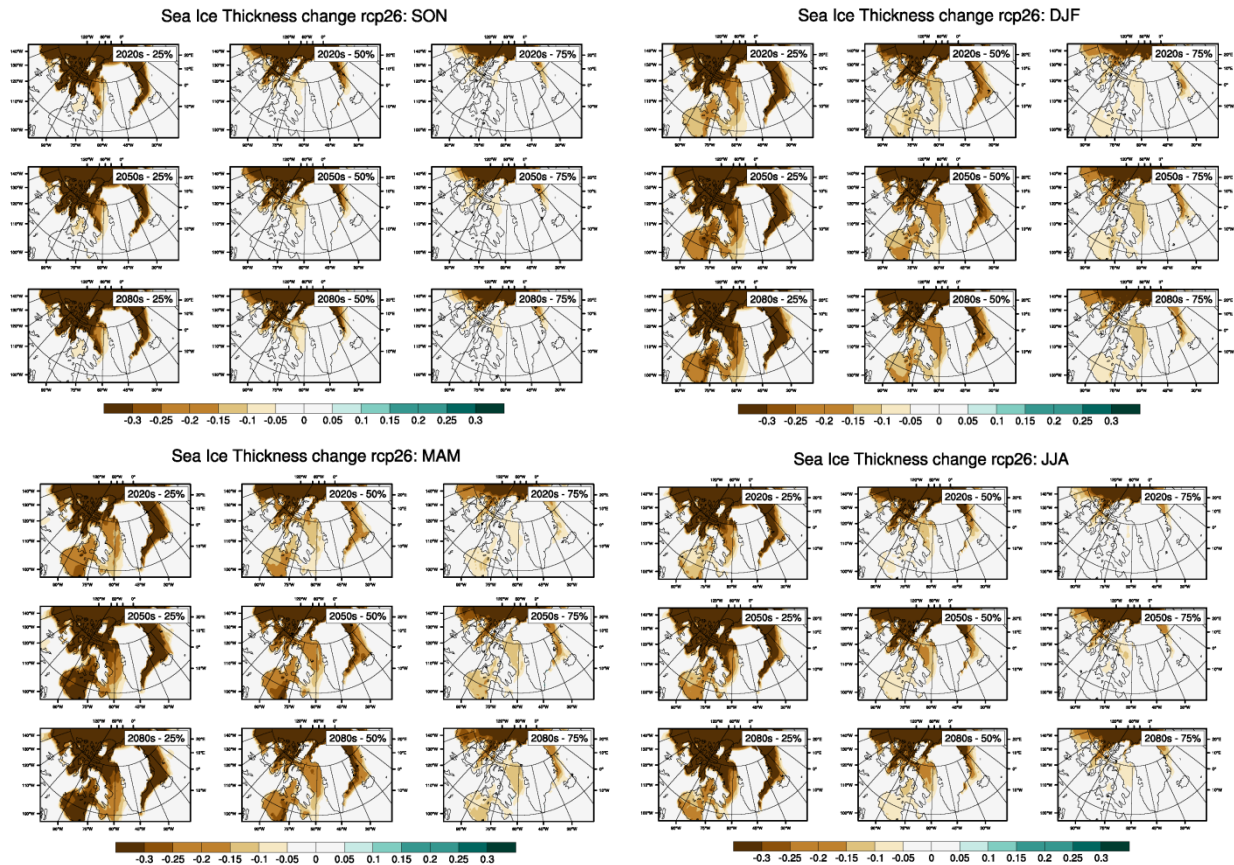


Figure SM3.18: 29 member CMIP5 multi-model projected change in sea-ice thickness (change in m relative to 1986-2005 average) for RCP2.6 scenario. Results are shown for four seasons and three periods in the future: 2016-2035 (labelled 2020s), 2046-2065 (labelled 2050s) and 2081-2100 (labelled 2080s), and illustrate the 25th, 50th and 75th percentile changes projected by the 29 CMIP5 models used (see BCB report for listing of models). [Prepared by Robin Rong, EC/CCCma]



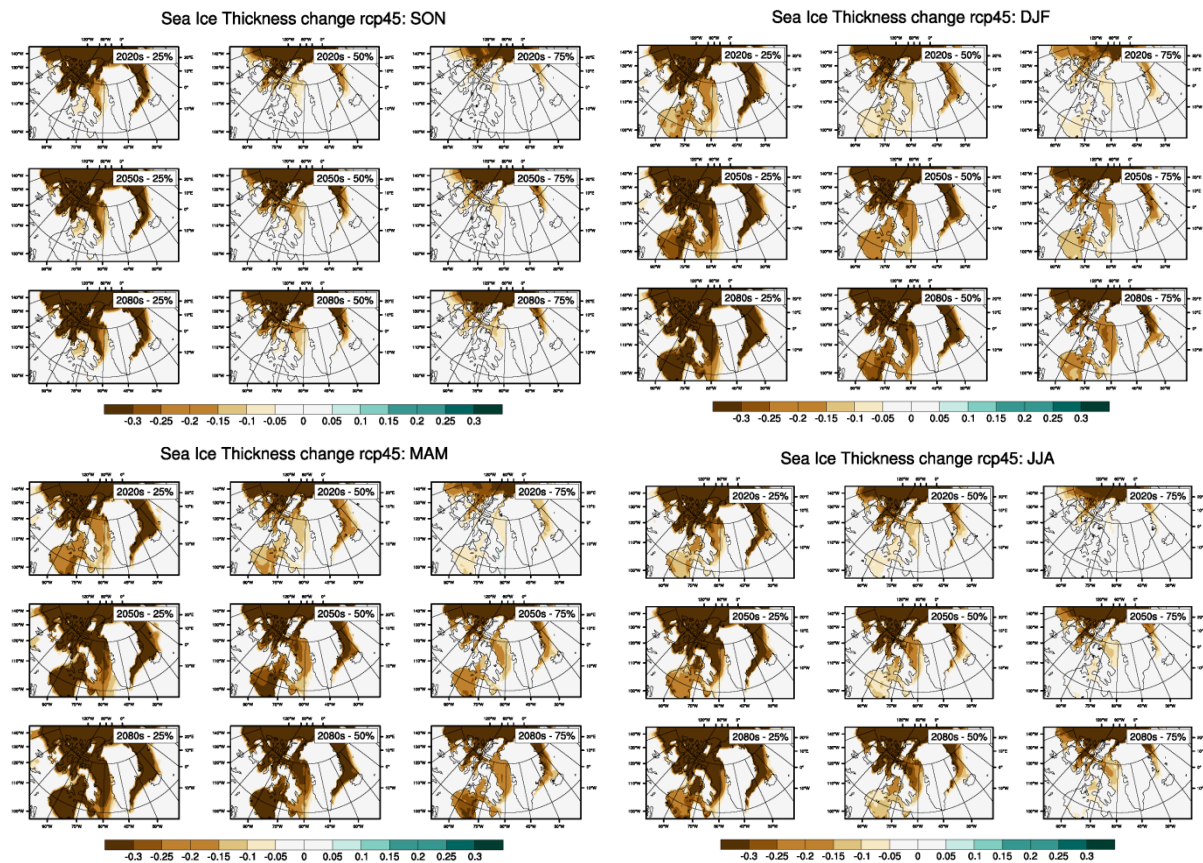


Figure SM3.19: same as Figure SM3.18 for RCP4.5 scenario. [Prepared by Robin Rong, EC/CCCma]

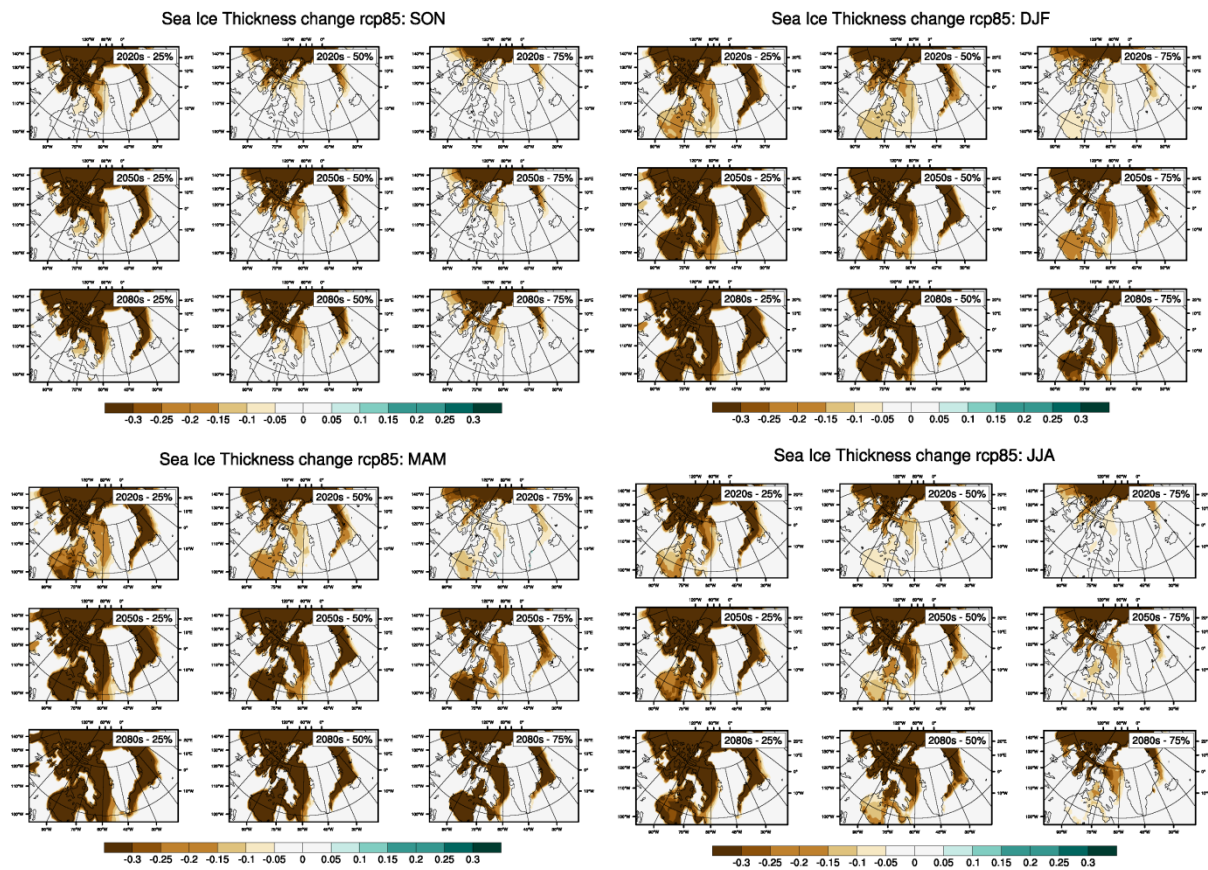


Figure SM3.20: same as Figure SM3.18 for RCP8.5 scenario. [Prepared by Robin Rong, EC/CCCma]

## References

- Barnes, E.A. and Polvani, L.M., 2015: CMIP5 Projections of Arctic Amplification, of the North American/North Atlantic Circulation, and of Their Relationship. *J. Climate*, 28, 5254–5271.
- Bengtsson, L., Hodges, K.I., Koumoutsaris, S., Zahn, M., and Keenlyside, N., 2011: The changing atmospheric water cycle in Polar Regions in a warmer climate. *Tellus A*, 63A, 907-920.
- Bintanja, R., and Selten, F.M., 2014: Future increases in Arctic precipitation linked to local evaporation and sea-ice retreat. *Nature*, Vol. 509, 479-482, doi:10.1038/nature13259.
- Bracegirdle, T.J., and Stephenson, D.B., 2013: On the Robustness of Emergent Constraints Used in Multimodel Climate Change Projections of Arctic Warming. *J. Climate*, 26, 669–678.
- Brown, R.D. and R.O. Braaten, 1998: Spatial and temporal variability of Canadian monthly snow depths, 1946-1995. *Atmosphere-Ocean*, 36: 37-45.
- Brown, R. And coauthors, 2016: Climate variability, trends and projected change for the Eastern Canadian Arctic. Chapter xx in ArcticNet IRIS-2 report (in press.)
- Brown, R. and coauthors, 2017: SWIPA update, Arctic Terrestrial Snow Cover (in press.)
- Curry, J.A., Schramm, J.L., Rossow, W.B., and Randall, D., 1996: Overview of Arctic Cloud and Radiation Characteristics. *J. Climate*, 9, 1731–1764.
- Davies, F.J., Renssen, H., and Goosse, H., 2014: The Arctic freshwater cycle during a naturally and an anthropogenically induced warm climate. *Clim. Dyn.*, 42, pp. 2099–2112, doi:10.1007/s00382-013-1849-y.
- Déry, S. J., and Wood, E. F. , 2005: Decreasing river discharge in northern Canada, *Geophys. Res. Lett.*, 32, L10401, doi:10.1029/2005GL022845.
- Eisenman, I., N. Untersteiner, and J. S. Wettlaufer (2007), On the reliability of simulated Arctic sea ice in global climate models, *Geophys. Res. Lett.*, 34, L10501, doi:10.1029/2007GL029914.
- English, J., A. Gettelman, and G. Henderson, 2015: Arctic Radiative Fluxes: Present-day biases and future projections in CMIP5 models. *J. Climate*. doi:10.1175/JCLI-D-14-00801.1, in press.
- Estilow, T. W., A. H. Young, and D. A. Robinson, 2015: A long-term Northern Hemisphere snow cover extent data record for climate studies and monitoring. *Earth System Science Data* 7.1: 137-142.
- Held, I. M., and Soden, B.J., 2006: Robust responses of the hydrological cycle to global warming. *J. Clim.*, vol. 19, pp. 5686–5699.
- IPCC, 2013: Annex I: Atlas of Global and Regional Climate Projections [van Oldenborgh, G.J., M. Collins, J. Arblaster, J.H. Christensen, J. Marotzke, S.B. Power, M. Rummukainen and T. Zhou (eds.)]. In: *Climate Change 2013: The Physical Science Basis. Contribution of Working Group I to the Fifth Assessment Report of the Intergovernmental Panel on Climate Change* [Stocker, T.F., D. Qin, G.-K. Plattner, M. Tignor, S.K.

Allen, J. Boschung, A. Nauels, Y. Xia, V. Bex and P.M. Midgley (eds.)). Cambridge University Press, Cambridge, United Kingdom and New York, NY, USA.

Kattsov, V.M., Walsh, J.E., Chapman, W.L., Govorkova, V.A., Pavlova, T.V., and Zhang, X., 2007: Simulation and Projection of Arctic Freshwater Budget Components by the IPCC AR4 Global Climate Models. *Journal of Hydrometeorology*, Vol. 8, Issue 3, 571-589.

Key, E.L., Minnett, P.J., and Jones, R.A., 2004: Cloud distributions over the coastal Arctic Ocean: surface-based and satellite observations. *Atmospheric Research*, 72, pp. 57 – 88.

Koenigk, T., Brodeau, L., Graversen, R.G., Karlsson, J., Svensson, G., Tjernström, M., Willén, U., and Wyser, K., 2013: Arctic climate change in 21st century CMIP5 simulations with EC-Earth, *Clim. Dyn.*, 40, pp. 2719–2743, doi:10.1007/s00382-012-1505-y.

Langen, P.L., Graversen, R.G., and Mauritsen, T., 2012: Separation of Contributions from Radiative Feedbacks to Polar Amplification on an Aquaplanet. *J. Climate*, 25, 3010–3024.

Liston, G. E., and C. A. Hiemstra, 2011: The Changing Cryosphere: Pan-Arctic Snow Trends (1979–2009). *J. Clim.*, 24, 5691–5712, doi:10.1175/JCLI-D-11-00081.1.

Muskett, R.R., and Romanovsky, V.E., 2009: Groundwater storage changes in Arctic permafrost watersheds from GRACE and in situ measurements. *Environ. Res. Lett.*, 4, doi:10.1088/1748-9326/4/4/045009.

Peterson, I., J. Hamilton, S. Prinsenberg, and R. Pettipas (2012), Wind-forcing of volume transport through Lancaster Sound, *J. Geophys. Res.*, 117, C11018, doi:10.1029/2012JC008140.

Pithan, F., and T. Mauritsen, 2014: Arctic amplification dominated by temperature feedbacks in contemporary climate models. *Nature Geoscience*, 7, 181–184, doi:10.1038/ngeo2071.

Screen, J.A., Simmonds, I., Deser, C., Tomas, R., 2013: The Atmospheric Response to Three Decades of Observed Arctic Sea Ice Loss. *J. Climate*, 26, 1230–1248

Serreze, M., and Barry, R., 2011: Processes and impacts of Arctic amplification: A research synthesis. *Global and Planetary Change*, 77, pp.85–96.

Taylor, P.C., Ming Cai, Aixue Hu, Jerry Meehl, Warren Washington, and Guang J. Zhang, 2013: A Decomposition of Feedback Contributions to Polar Warming Amplification. *J. Climate*, 26, 7023–7043.

Vavrus, S., Waliser, D., Schweiger, A., and Francis, J., 2009: Simulations of 20th and 21st century Arctic cloud amount in the global climate models assessed in the IPCC AR4. *Clim. Dyn.*, 33, pp. 1099–1115, doi:10.1007/s00382-008-0475-6.

Vihma, T., Screen, J., Tjernström, M., Newton, B., Zhang, X., Popova, V., Deser, C., Holland, M. and Prowse, T., 2015: The atmospheric role in the Arctic water cycle: A review on processes, past and future changes, and their impacts. *J. Geophys. Res. Biogeosci.*, 121, 586–620, doi:10.1002/2015JG003132.

Yu, Y., H. Stern, C. Fowler, F. Fetterer, and J. Maslanik, 2014: Interannual Variability of Arctic Landfast Ice between 1976 and 2007. *J. Climate*, 27, 227–243. doi: <http://dx.doi.org/10.1175/JCLI-D-13-00178.1>

Zhang, X., He, J., Zhang, J., Polyakov, I., Gerdes, R., Inoue, J., and Wu, P., 2012: Enhanced poleward moisture transport and amplified northern high-latitude wetting trend. *Nature Climate Change*, vol. 3, doi: 10.1038/nclimate1631.